Korean J. Chem. Eng., 36(2), 210-216 (2019)
DOI: 10.1007/s11814-018-0209-3

pISSN: 0256-1115
eISSN: 1975-7220

Effect of acidic properties of hierarchical HZSM-5 on the product distribution in methanol conversion to gasoline

Huiwen Huang, Hui Zhu, Qiang Zhang, and Chunyi Li†

State Key Laboratory of Heavy Oil Processing, China University of Petroleum (East China), Qingdao 266580, China
(*Received 25 October 2018 • accepted 12 December 2018*)

Abstract−Hierarchical ZSM-5 zeolites with different SiO_2/Al_2O_3 ratio but similar crystal size were directly synthesized by a single-template hydrothermal method, and the intrinsic effect of acidic properties on their catalytic performance in methanol to gasoline (MTG) reaction was comprehensively investigated. The physicochemical properties of HZSM-5 zeolites were characterized by XRD, N_2 adsorption-desorption, SEM, NH_3-TPD, FTIR, and TGA techniques. The results show good linear correlations between the yields of gasoline components and the relative content of Brønsted acid sites, and the hierarchical HZSM-5 zeolite with SiO_2/Al_2O_3 molar ratio of 200 was firstly found to exhibit high reactivity, excellent product distribution and superior stability in MTG reaction, which can be attributed to its appropriate acid distribution with moderate Brønsted acid sites and proper B/L ratio, predominantly promoting gasoline range hydrocarbons production and inhibiting side reactions.

Keywords: Methanol, Gasoline, Hierarchical HZSM-5 Zeolites, Acidity, Deactivation

INTRODUCTION

The methanol to gasoline (MTG) process is an excellent way to produce high-octane gasoline, since methanol can be readily produced via synthesis gas from multifarious sources like coal, natural gas and biomass [1-7]. Due to the shortage of crude oil in recent years, the MTG process has received considerable attention. In the 1970s, Exxon Mobil was the first to discover and develop the MTG technology using a HZSM-5 catalyst, which is widely accepted so far to be the most effective catalyst for this process [3-9]. The activity and selectivity of HZSM-5 catalysts depend heavily on their crystal size, channel structure and acidic properties under the optimized operating conditions [2,5-10]. At present, the major problem faced by the MTG reaction is the rapid deactivation of HZSM-5 catalysts, which yield more aromatics and carbon deposits with less C_5-C_{10} alkanes [8]. Therefore, continuing research and development efforts have been devoted for the improvement of catalytic stability and gasoline composition of HZSM-5 catalysts.

Bjørgen et al. [9] reported that the selectivity to alkanes in MTG reaction was improved by the formation of accessible intracrystalline mesopores in desilicated HZSM-5 catalysts with NaOH solution. The post-processes of ZSM-5 catalysts in $CaCO_3$, Na_2CO_3 and NaOH solutions lead to higher yield of gasoline range hydrocarbons and prolonged lifetime [10]. Campbell et al. [11] found that the lifetime of dealuminated HZSM-5 catalysts caused by water was increased significantly, and they concluded that although up to ca. 90 wt% of the framework aluminum considered to be the active sites was lost in the dealumination process, the ZSM-5 samples still performed well in MTG reaction. Moreover, it also has been reported that the generated sites induced by lowering aluminum content at the outer shell of ZSM-5 zeolites were highly selective to gasoline range hydrocarbons [6]. Hence, it is significantly needed to study the hierarchically high-silica HZSM-5 catalysts for MTG reaction.

Nowadays, hierarchical ZSM-5 zeolites can be obtained by several strategies, including the aforementioned post-treatment approaches of dealumination and desilication [9,12-14], soft-template and hard-template synthesis methods [15-19]. Even though these means are effective and improved catalytic performance is obtained in many reactions, they also have some disadvantages. Specifically, the chemical dissolution in the post-treatment methods often leads to great losses of the zeolites. The usages of expensive templates or troublesome preprocessing steps are unavoidable in the soft-template methods. For the hard-template methods, the uncontrolled generation of structural defects caused by high temperature calcination is detrimental to the catalytic properties of ZSM-5 zeolites. Thus, it is quite necessary for a developed synthetic route for hierarchical ZSM-5 zeolites based on simplicity, economy and reproducibility. In addition, the crystal size of ZSM-5 zeolites has been regarded as a key factor in determining their catalytic performance in an MTG reaction [20]. However, it is challenging to synthesize ZSM-5 zeolites with the same crystal size but different SiO_2/Al_2O_3 ratio because of the interplay between SiO_2/Al_2O_3 ratio and crystal size.

To the best of our knowledge, although several papers are available on monitoring the changes of methanol conversion and product distribution with acidity over HZSM-5 catalysts in many reactions, the detailed literature focused on the intrinsic effect of acidity induced by SiO_2/Al_2O_3 ratio on the catalytic performance of hierarchically high-silica HZSM-5 archetype catalysts independent of crystal size in MTG reaction is still lacking. In this contribution, we report a facile method for the direct synthesis of hierarchical HZSM-5 zeo-

†To whom correspondence should be addressed.
E-mail: chyli_upc@126.com

lites with almost identical crystal size but different SiO_2/Al_2O_3 ratio, and without the need of additional templates. Furthermore, the catalytic performance of the synthesized samples is evaluated in MTG reaction, and the relationship between acid properties and catalytic behaviors is given in detail, aiming at exploring a favorable MTG catalyst.

EXPERIMENTAL

1. Catalyst Preparation

Hierarchal ZSM-5 zeolites with different SiO_2/Al_2O_3 molar ratio but similar crystal size were prepared by a single-template hydrothermal crystallization method; details about the preparation procedures are given in the Supplementary Material.

2. Catalyst Characterization

The samples were characterized by X-ray diffraction, scanning electron microscope, nitrogen adsorption-desorption, temperature-programmed desorption of ammonia, Fourier-transform infrared spectroscopy and thermo-gravimetric analysis experiments; detailed descriptions of these characterizations are presented in the Supplementary Material.

3. Catalytic Evaluation

The MTG reaction was carried out at 375 °C in a fixed-bed tubular stainless steel microreactor under atmospheric pressure. For each test, 3.0 g zeolite with particle size of 40-60 mesh was loaded into the center of the reactor. Prior to reaction, the zeolite was activated at 500 °C in flowing nitrogen (20 mL/min) for 30 min and cooled to the reaction temperature. Then, the liquid methanol with weight hourly space velocity of 3.26 h^{-1} was fed by an HPLC infusion pump with nitrogen (20 mL/min) as carrier gas into the reactor. The reactor exit stream was separated into gaseous and liquid products using an ice-cooled condenser. The analysis method and instruments for the products are described in the Supplementary Material.

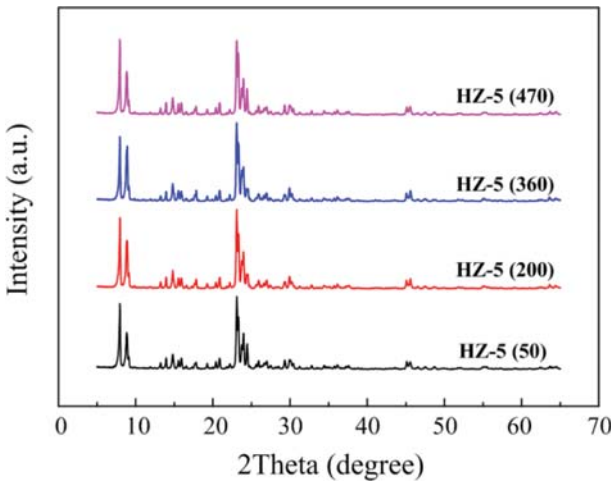

Fig. 1. XRD patterns of HZSM-5 zeolites.

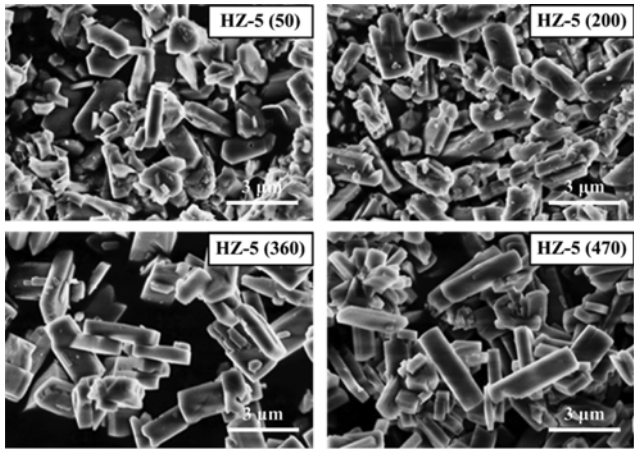

Fig. 2. SEM images of HZSM-5 zeolites.

RESULTS AND DISCUSSION

1. Textural Properties of HZSM-5 Zeolites

XRD patterns of HZSM-5 zeolites are shown in Fig. 1, and all samples exhibit the typical diffraction peaks of intrinsic MFI structure. Taking HZ-5 (470) zeolite as the basic standard, the relative crystallinity of the other samples based on the intensities of the peaks at 2θ=8-9° and 22-25° was calculated and listed in Table 1. Apparently, all HZSM-5 zeolites demonstrate high crystallinity, confirming the highly crystalline MFI structure of the samples used in this study. The representative SEM images depicted in Fig. 2 clearly show that all HZSM-5 zeolites display similar morphology of pris-

Table 1. Textural properties of HZSM-5 zeolites

Samples	S_{BET}[a] (m^2/g)	S_{Mirco}[c] (m^2/g)	V_{Total}[b] (cm^3/g)	V_{Mirco}[c] (cm^3/g)	Relative crystallinity[d] (×100%)	Crystal size[e] (μm)
HZ-5 (50)	395.2	370.1	0.19	0.13	96.4	~2
HZ-5 (200)	401.3	374.8	0.21	0.15	98.7	~2
HZ-5 (360)	404.9	377.9	0.19	0.14	97.1	~3
HZ-5 (470)	412.0	380.7	0.20	0.14	100.0	~3

[a]BET surface area was obtained by the BET method

[b]Total pore volume was estimated from the nitrogen adsorbed amount at p/p_0=0.99

[c]Both the micropore surface area and volume were determined by the *t*-plot method

[d]Relative crystallinity was estimated by comparing the diffraction peak heights of 2θ=8-9° and 22-25° with that of the reference sample

[e]Crystal size was estimated from SEM image

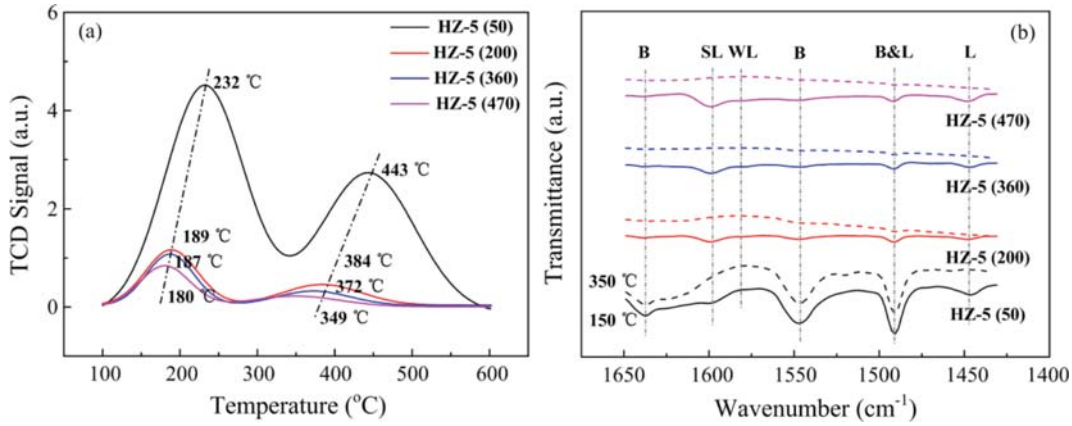

Fig. 3. NH_3-TPD profiles (a) and Py-FTIR spectra (b) of HZSM-5 zeolites.

matic crystals, which is the characteristic for the MFI structure. It can also be seen that the average crystal size of the samples is about 2-3 μm (Table 1), with some smaller crystallites and larger agglomerates. As shown in Fig. S1, the nitrogen isotherms of all samples are a combination of type I and IV with high adsorption volume at a very low relative pressure and a distinct hysteresis loop, which is typical for microporous materials with significant mesopores [21]. The pore size distribution profiles (Fig. S2) further confirm the micro-mesoporous dual model structure of these samples, and the mesopores in these samples can be attributed to the crystals agglomeration with an inter-particle space of 2-4 nm. In addition, all HZSM-5 zeolites have similar surface areas and pore volumes, as summarized in Table 1.

The acidic properties of the samples were determined by NH_3-TPD and Py-FTIR techniques. As shown in Fig. 3(a), NH_3-TPD profiles of all samples exhibit two desorption peaks, that is, a low temperature peak at 100-350 °C and a high-temperature peak at 350-600 °C, which corresponds to the desorption of NH_3 from the weak and strong acid sites on catalyst surfaces, respectively. It can be observed that the desorption peaks of NH_3 for both the weak and strong acid sites shift towards lower temperatures with the increase in SiO_2/Al_2O_3 ratio, which is accompanied by a pronounced decrease in acid density (Table 2). These are primarily caused by the decrease of aluminum content in the samples [22]. That is, the strength and density of the acid sites on HZSM-5 zeolites are correlated well with their SiO_2/Al_2O_3 ratio.

Table 2. Acidity analysis of HZSM-5 zeolites

Samples	Acid density (mmol NH_3/g)			B/L[c]
	Weak[a]	Strong[b]	Total	
HZ-5 (50)	0.531	0.389	0.920	7.48
HZ-5 (200)	0.083	0.047	0.130	2.22
HZ-5 (360)	0.071	0.030	0.101	1.01
HZ-5 (470)	0.058	0.027	0.085	0.50

[a]Calculated from the integral area at 100-350 °C of NH_3-TPD profiles
[b]Calculated from the integral area at 350-600 °C of NH_3-TPD profiles
[c]Obtained from the areas of the bands at 1,550 cm^{-1} and 1,455 cm^{-1} in Py-FTIR spectra

Py-FTIR spectra of HZSM-5 zeolites in the region of 1,650-1,400 cm^{-1} are presented in Fig. 3(b). The bands at around 1,540 cm^{-1} and 1,450 cm^{-1} are assigned to the vibration modes of pyridinium ions chemisorbed on Brønsted acid sites and coordinatively bound pyridine interacting with Lewis acid sites, respectively. As shown in Fig. 3(b), the amount of Brønsted acid sites declines sharply with increasing SiO_2/Al_2O_3 ratio, while the change of Lewis acid sites is complex. Compared with HZ-5 (50) zeolite, HZ-5 (200) zeolite contains fewer Lewis acid sites, but with a further increase in SiO_2/Al_2O_3 ratio, the amount of Lewis acid sites increases slightly. As a result, the values of B/L ratio obtained from the areas of the corresponding acid sites in the Py-FTIR spectra decrease strikingly with increasing SiO_2/Al_2O_3 ratio (Table 2) [23]. Furthermore, it should be noted that the strong acid sites on HZ-5 (x) samples are mainly Brønsted acid sites (Fig. 3(b)). Combining the results of NH_3-TPD and Py-FTIR of HZSM-5 zeolites, it can be concluded that with an increase in the amount of Brønsted acid sites, the number strong acid sites also increases.

2. Catalytic Performance of HZSM-5 Zeolites in MTG Reaction

Methanol conversion and product distribution of all HZSM-5 zeolites in MTG reaction at 2 h on stream are listed in Table 3. All samples evidently display high activity for MTG reaction with almost 100 wt% of methanol conversion, which can be attributed to the intrinsic MFI structure with high crystallinity of the zeolites and the high concentration of strong acid sites on their surfaces [24, 25]. As for product distribution, all zeolites yield almost the same amount of dry gas (2.3-2.7 wt%), C_3-C_4 hydrocarbons (13.7-16.0 wt%) and gasoline fraction (25.0-27.7 wt%). In spite of this, the compositions of the above three components significantly change with increasing SiO_2/Al_2O_3 ratio under our reaction conditions. Specifically, methane and ethene are always the main components of dry gas for HZSM-5 zeolites with different SiO_2/Al_2O_3 ratio but with different variation tendency. For high-silica HZSM-5 zeolites, alkenes are the dominant components of liquefied petroleum gas; instead, alkanes account for larger proportion of liquefied petroleum gas for HZ-5 (50) zeolite. Together, a small amount of methane is detected for all HZSM-5 samples (<1.2 wt%), and the yield of C_2-C_4 hydrocarbons as major gaseous components remains relatively constant (ca. 16.0 wt%). In addition, there is a significant

Table 3. MTG results of HZSM-5 catalysts at 2 h on stream

Catalysts		HZ-5 (50)	HZ-5 (200)	HZ-5 (360)	HZ-5 (470)
Conversion (wt%)		99.99	99.95	99.90	99.95
Yield (wt%)	Dry gas	2.72	2.66	2.64	2.29
	LPG	16.01	13.80	14.24	13.65
	Gasoline	24.96	27.23	26.78	27.74
	Durene	0.65	0.81	0.90	0.07
CH_4/Dry gas (%)		43.95	11.42	10.80	11.38
C_2H_4/Dry gas (%)		17.52	78.47	85.35	84.35
C_3H_6/LPG (%)		4.18	29.05	42.98	40.47
C_4H_8/LPG (%)		2.14	21.46	36.48	36.04
Gasoline composition (%)	iso-Paraffins	7.13	18.05	22.62	24.96
	n-Paraffins	2.49	3.67	3.03	4.63
	Olefins	0.39	16.82	34.08	44.89
	Naphthenes	1.56	10.39	11.73	12.80
	Aromatics	88.43	51.07	28.54	12.73
Benzene/Aromatics (%)		6.66	1.92	6.24	19.35
Toluene/Aromatics (%)		34.16	18.05	10.49	23.04
Xylene/Aromatics (%)		39.70	41.90	37.74	34.69

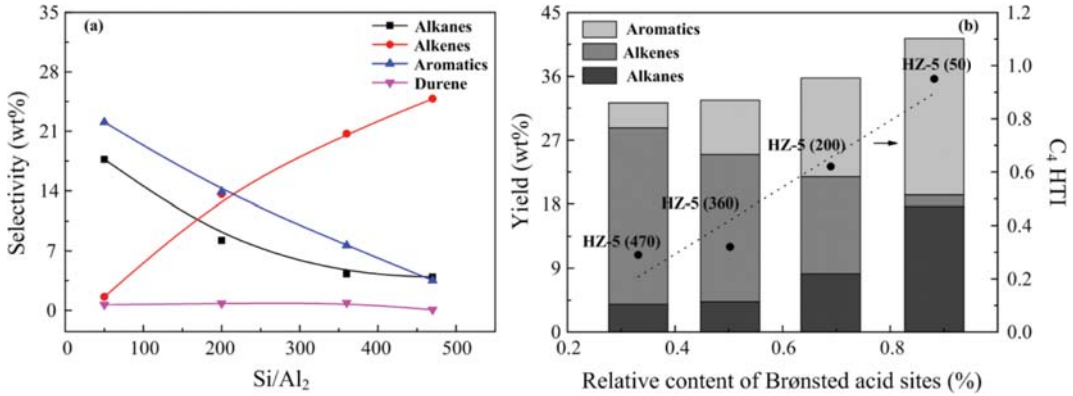

Fig. 4. Product selectivity (a) C_4 HTI and product yield (b) over HZSM-5 catalysts.

difference in the composition of gasoline fraction. With an increase in SiO_2/Al_2O_3 ratio, the content of aromatics decreases gradually, whereas the content of paraffins, olefins, and naphthenes increases to varying degrees. Besides, the aromatic components are A_6-A_{12} hydrocarbons, with A_8 aromatics being the major component. Compared with the reported data (1.7-4.7 wt%), an important effect of hierarchical HZSM-5 zeolites is a remarkable decrease in durene selectivity [Fig. 4(a)] (<1.0 wt%), since a concentration of durene in gasoline higher than 5.0 wt% will cause rough engine operation [26].

Since the MTG reaction is an acid-catalyzed and shape-selective reaction, and the HZSM-5 zeolites with different SiO_2/Al_2O_3 ratio used in this study have similar textural properties, the above differences in product distribution must result from the different nature of the acid sites on catalyst surfaces [27-29]. Although the strong acid sites are essential for hydrocarbons production from methanol, they can also facilitate the formation of aromatics and coke by hydrogen transfer, alkylation and oligomerization reactions, while the weak acid sites are conducive to the initial activity of methanol as well as alkylation and methylation reactions [27-31]. Accordingly, the increase in alkene selectivity and the decrease in the selectivity to alkanes and aromatics with increasing $SiO_2/$

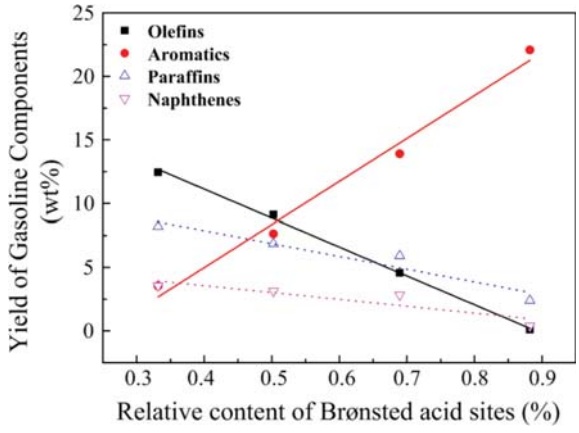

Fig. 5. Yield of gasoline components with the relative content of Brønsted acid sites of HZSM-5 zeolites.

Al_2O_3 ratio can be ascribed to the reduced probability for secondary reactions like cyclization and hydrogen transfer on the strong acid sites of HZSM-5 zeolites [Fig. 4(a)].

Fig. 5 shows the yield curves of gasoline components with the relative content of Brønsted acid sites. It is evident that there are good linear relations between the yields of olefins, aromatics, paraffins, and naphthenes in gasoline fraction and the relative content of Brønsted acid sites over different zeolites. That is, the aromatics yield increases monotonically with the increasing relative content of Brønsted acid sites, whereas the yields of paraffins, olefins and naphthenes show the opposite trend, implying that a higher density of Brønsted acid sites is more conducive to the formation of aromatics rather than olefins, etc. As a result, the aromatic yield on HZ-5 (50) catalyst is six-times higher than that on HZ-5 (470) catalyst (Table 3).

The conversion of methanol to hydrocarbons (MTH) is composed of a series of reactions, in which methanol is first dehydrated to DME and water, and then methanol and DME are converted to light olefins [1,2]. Later, the light olefins react to form higher olefins, alkanes, and aromatics through hydrogen transfer, cyclization and oligomerization reactions (Scheme 1). The Brønsted acid sites are reported to be the active centers for oligomerization, hydrogen transfer and cracking reactions, while the alkylation and dehydrogenation reactions occur mainly on the Lewis acid sites [32,33]. Liu et al. [33] found that a small fraction of Brønsted acid sites is sufficient for the transformation of methanol to various gasoline range hydrocarbons, which is in line with the opinion of Campbell et al. [11], and the redundant Brønsted acid sites would lead to the formation of carbonaceous deposits [33]. Thus, the HZSM-5 catalysts with an appropriate acid distribution of moderate Brønsted acid sites and proper B/L ratio ought to exhibit excellent performance in MTG reaction. The hydrogen transfer reaction, which serves as a connection between the primary products (ethene and propene) and the secondary products (higher olefins, alkanes, and aromatics), can be used to further elaborate the above reaction results. In general, the extent of hydrogen transfer reaction over the catalysts can be reflected by C_4 hydrogen transfer index (C_4 HTI), which characterizes the ratio between the yield of butane and the total C_4 hydrocarbons [28]. As expected, the increasing trend between the C_4 HTI and the relative content of Brønsted acid sites indicates that the hydrogen transfer reaction of light olefins to alkanes and aromatics is strongly suppressed by the decreased content of Brønsted acid sites, which results in the reaction results as presented in Fig. 4(b).

From the above observations, the HZ-5 (200) zeolite exhibits excellent catalytic activity for MTG reaction compared with conventional HZSM-5 catalysts with the optimal gasoline composition (an appropriate content of aromatics, primarily straight and branched aliphatics), which is rich in desired toluene and xylene components and low content of undesired benzene (Table 3). Meanwhile, it also shows high selectivity to light olefins. Though the activity of HZ-5 (50) is also high, it demonstrates low selectivity to C_5-C_{10} alkanes with high yield of aromatics and few light olefins. Similarly, the low content of aromatics with high yield of olefins obtained on HZ-5

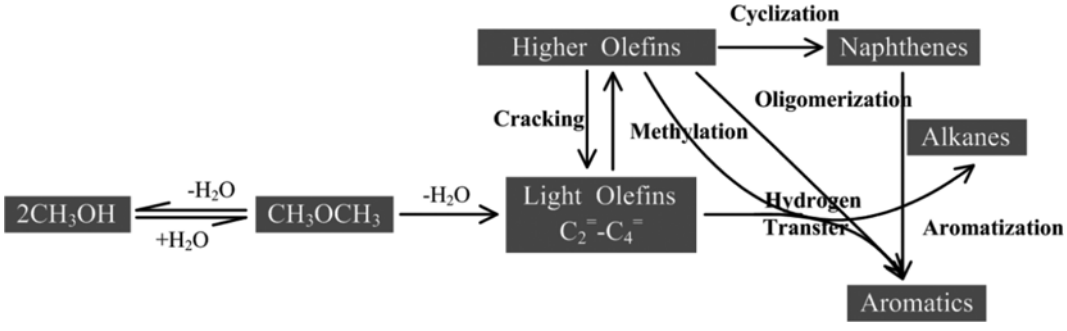

Scheme 1. Proposed reaction pathways for methanol conversion over HZSM-5 zeolites.

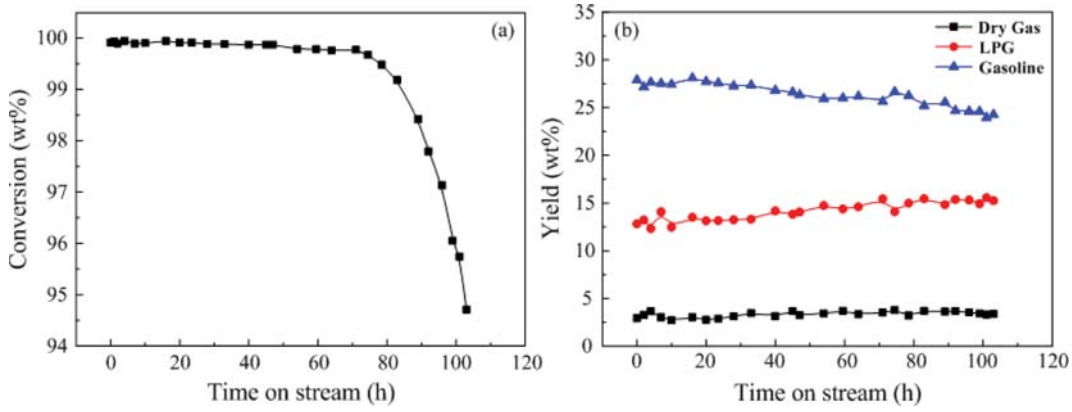

Fig. 6. Methanol conversion (a) and product distribution (b) of HZ-5 (200) catalyst versus time on stream.

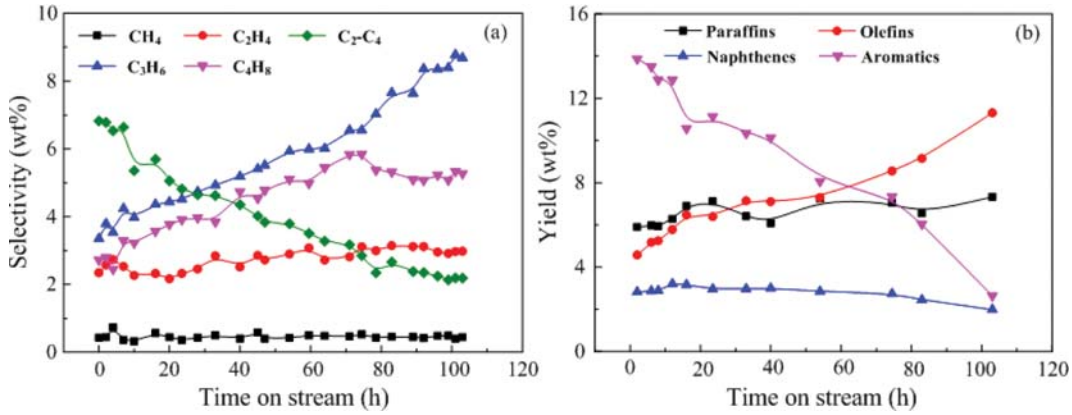

Fig. 7. Product selectivity (a) and yield of gasoline components (b) over HZ-5 (200) catalyst versus time on stream.

(360) and HZ-5 (470) catalysts indicates their unsuitability for MTG reaction. The above results imply that the catalytic performance of HZSM-5 catalysts in MTG reaction is closely associated with their acidic properties, and the proper B/L ratio contributes to the production of gasoline range hydrocarbons with suitable distribution of by-products. Note that the catalytic stability of HZSM-5 catalysts is still a major problem that needs to be overcome due to its rapid deactivation by carbon deposition [34,35]. Therefore, the stability of HZ-5 (200) catalyst in MTG reaction is investigated below.

3. Catalytic Stability of HZ-5 (200) Zeolite in MTG Reaction

Methanol conversion and product distribution as a function of time on stream for MTG reaction over HZ-5 (200) zeolite are illustrated in Fig. 6. During the whole reaction time of 103 h, the conversion of methanol drops slightly from 100 wt% to 94.7 wt% with an abrupt decline at 89 h, which is due to the reduced number of available acid sites caused by coke deposition during the reaction. Since the acid sites not only provide the active centers for methanol conversion and hydrocarbon production, but also are responsible for coke formation, when the coke deposits accumulate to some extent, it will block the pores of HZ-5 (200) zeolite and subsequently lead to a sharp deactivation [30]. TGA measurement of the coked HZ-5 (200) catalyst shows a weight loss of 7.64 wt% after 103 h on stream; specifically, the average rate of coke formation on HZ-5 (200) is only 0.07 mg/h (Fig. S3). Thus, the HZ-5 (200) catalyst demonstrates high activity and long-time stability for the MTG reaction, which can be ascribed to the appropriate concentration and strength of acid sites on its surfaces, improving its methanol conversion capacity and qualifying itself for good durability for carbon deposition.

In terms of product distribution over HZ-5 (200) catalyst with time on stream, the yield of dry gas is almost unchanged, but the yield of gasoline is decreased, which is accompanied by a slight increase in the yield of C_3-C_4 hydrocarbons, as displayed in Fig. 6(b). As mentioned, the reaction of methanol conversion over HZSM-5 zeolites is an acid-catalyzed consecutive process. Accordingly, the changes in product distribution can be attributed to the changes in acid properties, resulting from the formation of coke, that is, the secondary reactions like hydrogen transfer and cyclization are effectively inhibited by the reduction of available acid sites induced by the continuous carbon deposition. As a result, the generation of gasoline-range hydrocarbons is suppressed, while the liquefied petroleum gas yield is increased.

Fig. 7 shows the product selectivity to C_1-C_4 hydrocarbons and the yield of gasoline components over HZ-5 (200) catalyst versus reaction time. Propene prevails as the primary gaseous product, and its selectivity increases monotonically with the reaction. The selectivity to butene increases first and then decreases. In comparison with propene and butene, the selectivity to ethene is relative low, and it presents little change during the reaction. Besides, HZ-5 (200) catalyst also exhibits low selectivity to methane and there is a trace amount of H_2 and no CO and CO_2 are detected in the gaseous product (not shown). In the case of gasoline components, there is no obvious change in the yields of paraffins and naphthenes, but the yield of olefins increases slightly, as a result, the aromatics yield decreases substantially with the reaction (Fig. 7(b)).

It is well known that the mechanism of MTH reaction on acidic zeolites is very complicated, and the dual-cycle mechanism has been widely recognized [28,29]. In this mechanism, ethene is produced from lower methylbenzenes followed by re-methylation (the aromatic-based cycle), whereas propene and higher olefins are formed from repeated methylation and cracking reactions involving only C_3^+ olefins (the alkene-based cycle). Based on the different roles of the strong and weak acid sites in MTG reaction, the strong acid sites are probably more favorable to the propagation of the aromatic-based cycle, whereas the weak acid sites are more conducive to the alkene-based cycle [27-29]. Therefore, the observed changes in product selectivity with reaction time are caused by the transformation of the dominant way in the dual-cycle mechanism.

The decline in acid density caused by carbon deposition with the reaction can greatly suppress the cyclization and hydrogen transfer reactions, leading to a decline in the yields of alkanes and aromatics (Fig. 7). As a result, the alkene-based cycle becomes dominant and more C_3-$C_4^=$ hydrocarbons are produced (Fig. 7(a)). On the contrary, in the initial reaction period, the aromatic-based cycle is the principal reaction pathway, and then more C_2-C_4 alkanes and aromatics are formed (Fig. 7). Besides, the so-called shape-selective effect also plays an important role in this reaction. With an increase in coke content, the free space in the cavities of the catalysts becomes smaller, and then the formation of large molecules is strongly inhibited due to pore confinement effects; consequently,

the alkene-based cycle dominates the reaction. Thus, HZ-5 (200) catalyst exhibits considerable activity and superior catalytic stability in MTG reaction, with high yield of gasoline-range hydrocarbons, good selectivity to light olefins and low carbon content. In short, it has the potential as a promising MTG catalyst for industrial application.

CONCLUSIONS

Four hierarchical HZSM-5 zeolites with different SiO_2/Al_2O_3 ratio, but of almost identical crystal size and structural properties, were successfully synthesized through a single-template hydrothermal method. The effect of acid properties on catalytic performance of these samples was thoroughly investigated in MTG reaction. The reaction results show that the catalytic performance of HZSM-5 zeolites in MTG reaction is closely related to their acidic properties, and there are good linear correlations between the yields of gasoline components and the relative content of Brønsted acid sites. Hierarchal HZSM-5 zeolite with SiO_2/Al_2O_3 molar ratio of 200 was firstly proven to exhibit excellent activity in MTG reaction, which can be ascribed to its appropriate acid distribution with moderate Brønsted acid sites and proper B/L ratio, favoring the formation of desirable gasoline range hydrocarbons with suitable by-products distribution.

ACKNOWLEDGEMENTS

This work was financially supported by the National Natural Science Foundation for Young Scholars of China (21406270).

SUPPORTING INFORMATION

Additional information as noted in the text. This information is available via the Internet at http://www.springer.com/chemistry/journal/11814.

REFERENCES

1. C. D. Chang and A. J. Silvestri, *J. Catal.*, **47**, 249 (1997).
2. M. Stöcker, *Micropor. Mesopor. Mater.*, **29**, 3 (1999).
3. X. Meng, H. Huang, Q. Zhang, C. Li and Q. Cui, *Korean J. Chem. Eng.*, **33**, 1239 (2016).
4. H. A. Zaidi and K. K. Pant, *Catal. Today*, **96**, 155 (2004).
5. H. A. Zaidi and K. K. Pant, *Korean J. Chem. Eng.*, **22**, 353 (2005).
6. H. A. Zaidi and K. K. Pant, *Ind. Eng. Chem. Res.*, **47**, 2970 (2008).
7. H. A. Zaidi and K. K. Pant, *Korean J. Chem. Eng.*, **27**, 1404 (2010).
8. Z. Di, C. Yang, X. Jiao, J. Li, J. Wu and D. Zhang, *Fuel*, **104**, 878 (2013).
9. M. Bjørgen, F. Joensen, M. S. Holm, U. Olsbye, K. P. Lillerud and S. Svelle, *Appl. Catal. A*, **345**, 43 (2008).
10. S. Fathi, M. Sohrabi and C. Falamaki, *Fuel*, **116**, 529 (2014).
11. S. M. Campbell, D. M. Bibby, J. M. Coddington and R. F. Howe, *J. Catal.*, **161**, 338 (1996).
12. J. C. Groen, J. A. Moulijn and J. Pérez-Ramírez, *Ind. Eng. Chem. Res.*, **46**, 4193 (2007).
13. J. C. Groen, J. A. Moulijn and J. Pérez-Ramírez, *Micropor. Mesopor. Mater.*, **87**, 153 (2005).
14. H. Zhao, J. Ma, Q. Zhang, Z. Liu and R. Li, *Ind. Eng. Chem. Res.*, **53**, 13810 (2014).
15. M. Choi, K. Na, J. Kim, Y. Sakamoto, O. Terasaki and R. Ryoo, *Nature*, **461**, 246 (2009).
16. K. Na, C. Jo, J. Kim, K. Cho, J. Jung, Y. Seo, R. J. Messinger, B. F. Chmelka and R. Ryoo, *Science*, **333**, 328 (2011).
17. F. S. Xiao, L. Wang, C. Yin, K. Lin, Y. Di, J. Li, R. Xu, D. S. Su, R. Schlögl, T. Yokoi and T. Tatsumi, *Angew. Chem.*, **118**, 3162 (2006).
18. Y. S. Tao, H. Kanoh and K. Kaneko, *J. Am. Chem. Soc.*, **125**, 6044 (2003).
19. C. J. H. Jacobsen, C. Madsen, J. Houzvicka, I. Schmidt and A. Carlsson, *J. Am. Chem. Soc.*, **122**, 7116 (2000).
20. A. A. Rownaghi, F. Rezaei and J. Hedlund, *Catal. Commun.*, **14**, 37 (2011).
21. M. Rostamizadeh and A. Taeb, *J. Ind. Eng. Chem.*, **27**, 297 (2015).
22. P. L. Benito, A. G. Gayubo, A. T. Aguayo, M. Olazar and J. Bilbao, *J. Chem. Technol. Biot.*, **66**, 183 (1996).
23. J. C. Védrine, A. Auroux, V. Bolis, P. Dejaifve, C. Naccache, P. Wierzchowski, E. G. Derouane, J. B. Nagy, J. P. Gilson, J. H. C. van Hooff and P. Jan, *J. Catal.*, **59**, 248 (1979).
24. I. Othman, R. M. Mohamed, I. A. Ibrahim and M. M. Mohamed, *Appl. Catal. A*, **299**, 95 (2006).
25. M. Firoozi, M. Baghalha and M. Asadi, *Catal. Commun.*, **10**, 1582 (2009).
26. C. D. Chang, J. C. Kuo, W. H. Lang, S. M. Jacob, J. J. Wise and A. J. Silvestri, *Ind. Eng. Chem. Process Des. Dev.*, **17**, 255 (1978).
27. M. Bjørgen, F. Joensen, K. P. Lillerud, U. Olsbye and S. Svelle, *Catal. Today*, **142**, 90 (2009).
28. M. Bjørgen, S. Svelle, F. Joensen, J. Nerlov, S. Kolboe, F. Bonino, L. Palumboc, S. Bordigac and U. Olsbye, *J. Catal.*, **249**, 195 (2007).
29. S. Svelle, F. Joensen, J. Nerlov, U. Olsbye, K. P. Lillerud, S. Kolboe and M. Bjørgen, *J. Am. Chem. Soc.*, **128**, 14770 (2006).
30. F. L. Bleken, T. V. Janssens, S. Svelle and U. Olsbye, *Micropor. Mesopor. Mater.*, **164**, 190 (2012).
31. H. Schulz, *Catal. Today*, **154**, 183 (2010).
32. R. Barthos, T. Bánsági, T. S. Zakar and F. Solymosi, *J. Catal.*, **247**, 368 (2007).
33. J. F. Liu, Y. Liu and L. F. Peng, *J. Mol. Catal. A Chem.*, **280**, 7 (2008).
34. K. Barbera, F. Bonino, S. Bordiga, T. V. Janssens and P. Beato, *J. Catal.*, **280**, 196 (2011).
35. U. V. Mentzel, K. T. Højholt, M. S. Holm, R. Fehrmann and P. Beato, *Appl. Catal. A*, **417**, 290 (2012).

Supporting Information

Effect of acidic properties of hierarchical HZSM-5 on the product distribution in methanol conversion to gasoline

Huiwen Huang, Hui Zhu, Qiang Zhang, and Chunyi Li†

State Key Laboratory of Heavy Oil Processing, China University of Petroleum (East China), Qingdao 266580, China
(*Received 25 October 2018 • accepted 12 December 2018*)

S1. EXPERIMENTAL

S1.1. Catalyst Preparation

In this study, hierarchal ZSM-5 zeolites with different SiO_2/Al_2O_3 molar ratio but similar crystal size were prepared by a single-template hydrothermal crystallization method. The synthesis was performed with industrial sodium silicate solution ($Na_2SiO_3 \cdot nH_2O$, 26.5 wt%) as silicon source, sodium aluminate ($NaAlO_2$, 41.0 wt%) as aluminum source and tetrapropylammonium bromide (TPABr, 99.0 wt%) as the template. Briefly, the molar composition of the mixture was $Na_2O : Al_2O_3 : SiO_2 : TPABr : H_2O = 1-y : y : 50 : 3 : 850$ (y=1, 0.25, 0.14, 0.11), and its pH was adjusted to 11 by drop wise addition of concentrated sulfuric acid. After being vigorously stirred at room temperature for at least 2 h, the sol-gel was transferred into a static stainless-steel autoclave and crystallized at 180 °C under autogeneous pressure for 8 h. Then, the synthesized products were filtered, washed, dried at 120 °C overnight and followed by calcination at 550 °C in air for 6 h. The parent ZSM-5 zeolites were turned into H-form by three consecutive ion-exchanges with 1 mol/L NH_4NO_3 solution at 80 °C for 2 h, dried at 120 °C, and calcined at 550 °C for 2 h. In this paper, the obtained HZSM-5 zeolites were denoted as HZ-5 (x), where x refers to the SiO_2/Al_2O_3 molar ratio (x=50, 200, 360, and 470). Prior to the reaction, all sample powders were pressed into wafers and subsequently crushed and sieved into 40-60 mesh particles.

S1.2. Catalyst Characterization

X-ray diffraction (XRD) patterns were obtained on an X'Pert PRO MPD diffractometer with monochromatic Cu Kα radiation (40 kV and 40 mA) in the 2θ range from 5° to 65° at a scanning speed of 2°/min.

Scanning electron microscope (SEM) images were examined by an S-4800 field emission scanning electron microscope without deposition of any conducting materials or layers.

Nitrogen adsorption-desorption isotherms were measured on a Quadrasorb SI instrument at liquid nitrogen temperature. Before the measurement, the zeolite samples were degassed at 300 °C for 6 h to ensure complete removal of adsorbed moisture. The total BET surface area was calculated by the Brunauer-Emmett-Teller (BET) equation and the total pore volume was estimated at the nitrogen relative pressure of 0.99. The micropore surface area and micropore volume were determined by the *t*-plot method.

Temperature-programmed desorption of ammonia (NH_3-TPD) was performed on a PCA-1200 chemisorption analyzer with an on-line thermal conductivity detector (TCD). In a typical analysis, about 200 mg sample of 40-60 mesh was initially pretreated at 600 °C for 1 h with flowing helium (30 mL/min), and then cooled down to 100 °C and saturated with NH_3. After these operations, the sample was purged with helium to remove the physically adsorbed NH_3 until a stable TPD signal was attained. Finally, the temperature of the sample was increased from 100 °C to 600 °C at a heat-

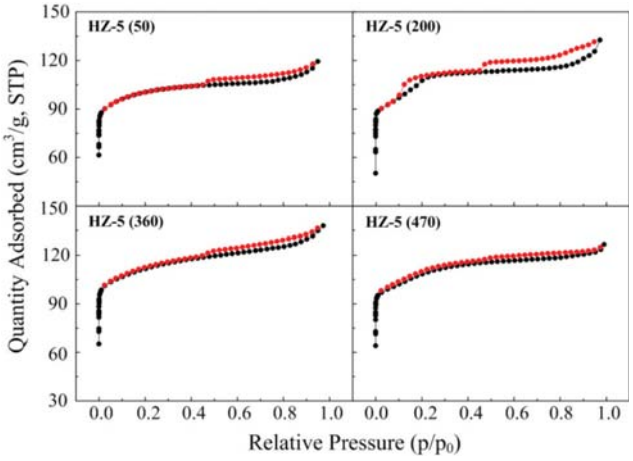

Fig. S1. N_2 adsorption-desorption isotherms of HZSM-5 zeolites.

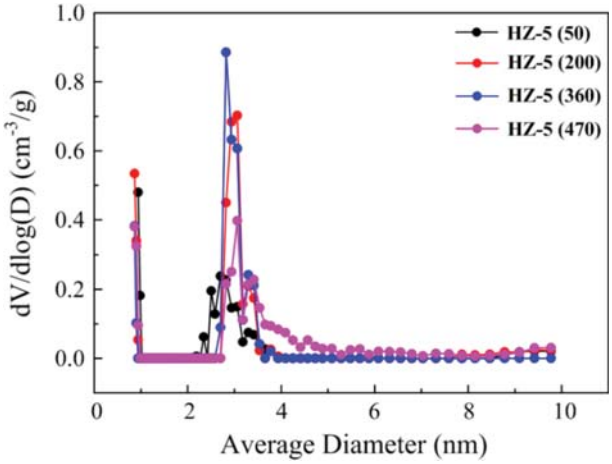

Fig. S2. Pore size distribution profiles of HZSM-5 zeolites.

ing rate of 10 °C/min.

Fourier-transform infrared spectroscopy (FTIR) measurements were conducted on a Tensor 27 FTIR instrument equipped with a MCT detector at the resolution of 4 cm^{-1} and 64 scans. The samples were first preheated at 150 °C for 12 h to remove the adsorbed impurities and adsorption of pyridine was performed by exposing the powders to the vapor pressure of pyridine at room temperate for 2 h. Then, the samples were evacuated at 150 °C and 1.0×10^{-3} kPa for 4 h, and the IR spectra were recorded at room temperature. The values of the integrated molar absorption coefficients used to determine the B/L ratio were 1.67 and 2.22 cm/μmol for Brønsted and Lewis acid sites, respectively [1].

Thermo-gravimetric analysis (TGA) was performed on a DTU-2A differential thermogravimetric analyzer. In a typical measurement, about 25 mg of spent catalyst was placed in a crucible, using Al_2O_3 as a reference. The temperature was raised from 50 °C to 850 °C at a heating rate of 10 °C/min.

S1.3. Catalytic Evaluation

The MTG reaction was carried out at 375 °C in a fixed-bed tubular stainless steel microreactor under atmospheric pressure. For each test, 3.0 g zeolite was loaded into the center of the reactor with an inner diameter of 12 mm. The reactor was heated electrically and the temperature was measured by an internal thermocouple, which was positioned in the center of the catalyst bed. Prior to the catalytic measurement, the zeolite was activated at 500 °C in flowing nitrogen (20 mL/min) for 30 min and cooled down to the reaction temperature. Then, the liquid methanol with weight hourly space velocity of 3.26 h^{-1} was fed by a HPLC infusion pump with nitrogen (20 mL/min) as carrier gas into the reactor. The reactor exit stream was separated into gaseous and liquid products using an ice-cooled condenser. The gaseous fractions were analyzed by a Bruker 450 gas chromatography (GC) with a flame ionization detector (FID) and two TCDs. The liquid products containing oil and aqueous phases were analyzed on a PerkinElmer PONA GC equipped with a FID and an Agilent 6820-GC fitted with HP-INNOWAX capillary column (30 m×0.32 mm×0.25 μm) and a FID, using ethanol as the internal standard for calibration.

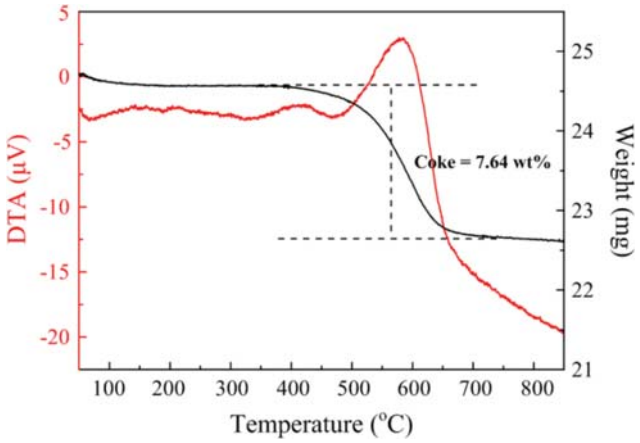

Fig. S3. TGA results of HZ-5 (200) zeolite.

The activity of the catalyst is expressed in terms of methanol conversion, which is calculated from the difference between the inlet and outlet masses of methanol and dimethyl ether (DME). Product yield is defined as the mass ratio of each product referred to the converted methanol and DME.

REFERENCE

1. C. A. Emeis, *J. Catal.*, **141**, 347 (1993).